Figure S1

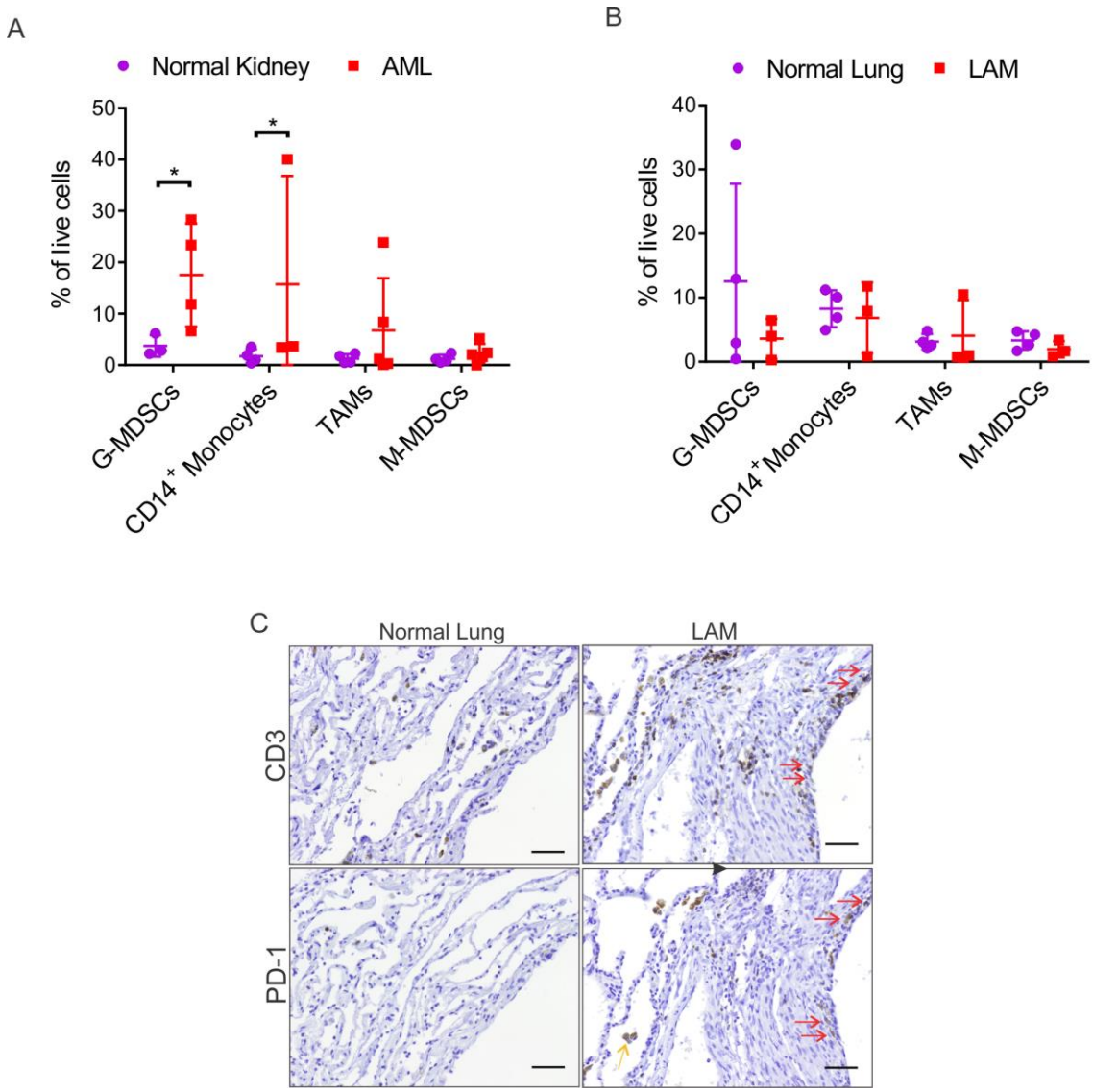

Supplemental Figure 1. G-MDSCs and CD14⁺ monocytes are increased in angiomyolipomas (AML). Multi-parametric flow cytometry data of AML (*n* = 3-5) and normal kidney (*n* = 3-4) **(A),** as well as lymphangioleiomyomatosis (LAM) (*n* = 3) and normal lung (*n* = 4) **(B)** indicating the frequency (%) of G-MDSC, monocytes, M-MDSCs and TAMs. Data are presented as mean ± SD. Statistical significance was determined by multiple *t*-test followed by Holm-Sidak post-test for multiple comparisons. * $p < 0.05$. **(C)** Representative immunohistochemistry for CD3 and PD-1 in serial sections of LAM (*n* = 10) and normal lung (*n* = 3). Red arrows indicate PD-1⁺ T cells. Scale bar: 50 µm.

Figure S2

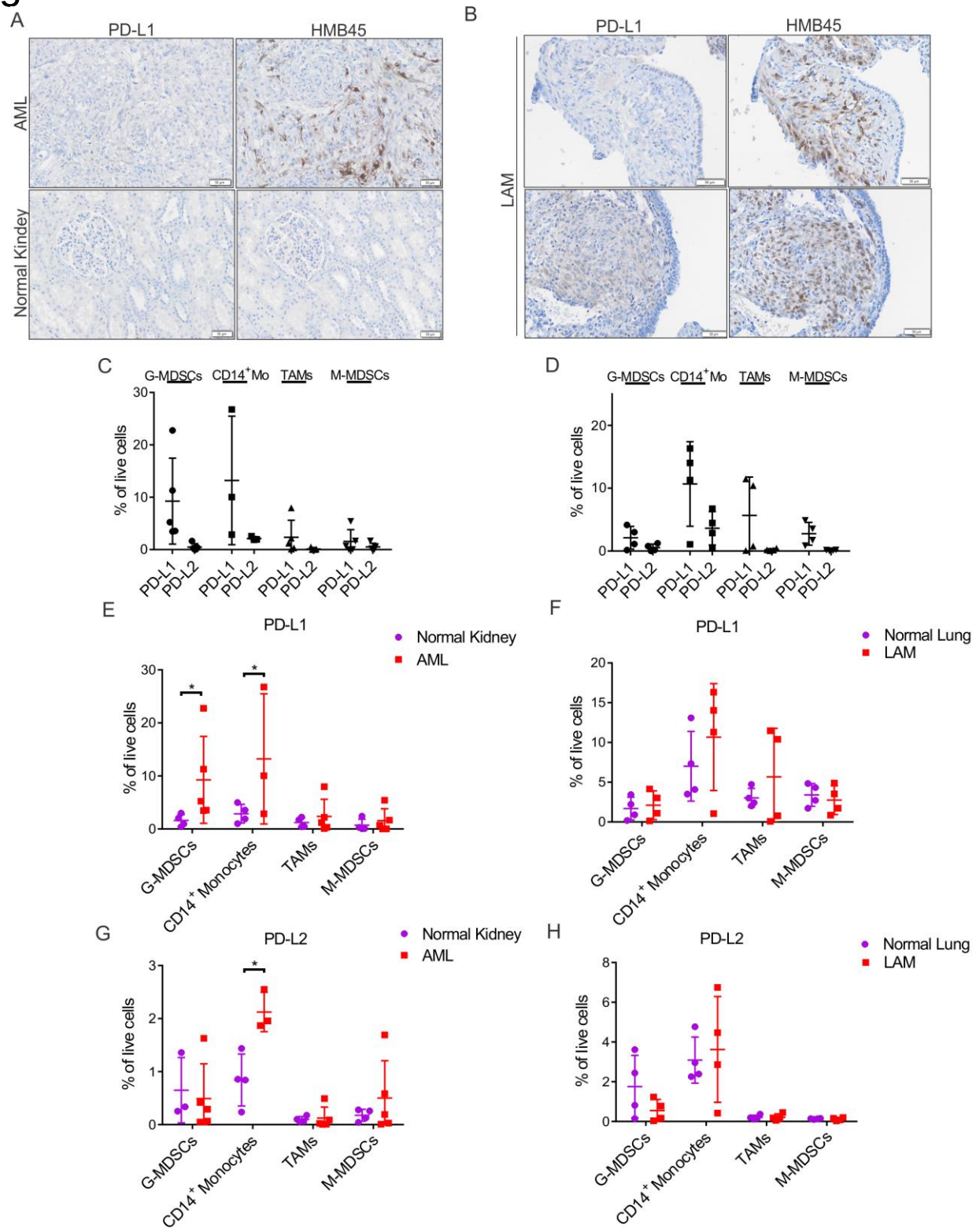

Supplemental Figure 2. PD-L1 expression is absent in angiomyolipomas (AML) and rarely present in lymphangioleiomyomatosis (LAM), but found on immune cells in the tumor microenvironment. (A) PD-L1 immunohistochemistry in AML (*n* = 10) and normal kidney (*n* = 4). Scale bar: 50 µm. **(B)** PD-L1 and HMB45 immunohistochemistry in LAM (*n* = 10) and normal lung (*n* = 3). Scale bar: 50 µm. Multiparametric flow cytometry analysis of PD-L1- and PD-L2-expressing G-MDSC, CD14⁺ monocytes, M-MDSCs and TAMs in AML (*n* = 3-5) **(C)** and LAM (*n* = 4) **(D)**. Multiparametric flow cytometry analysis of PD-L1-expressing G-MDSC, CD14⁺ monocytes, M-MDSCs and TAMs in AML (*n* = 3-5) versus normal kidney (*n* = 4) **(E),** and in LAM (*n* = 4) versus normal lung (*n* = 4) **(F)**. Multiparametric flow cytometry analysis of PD-L2-expressing G-MDSC, CD14⁺ monocytes, M-MDSCs and TAMs in AML (*n* = 3-5) versus normal kidney **(G),** and in LAM (*n* = 4) versus normal lung (*n* = 4) **(H)**. Data are presented as mean ± SD. Statistical significance was determined by multiple *t*-test followed by Holm-Sidak post-test for multiple comparisons. * $p < 0.05$.

Figure S3

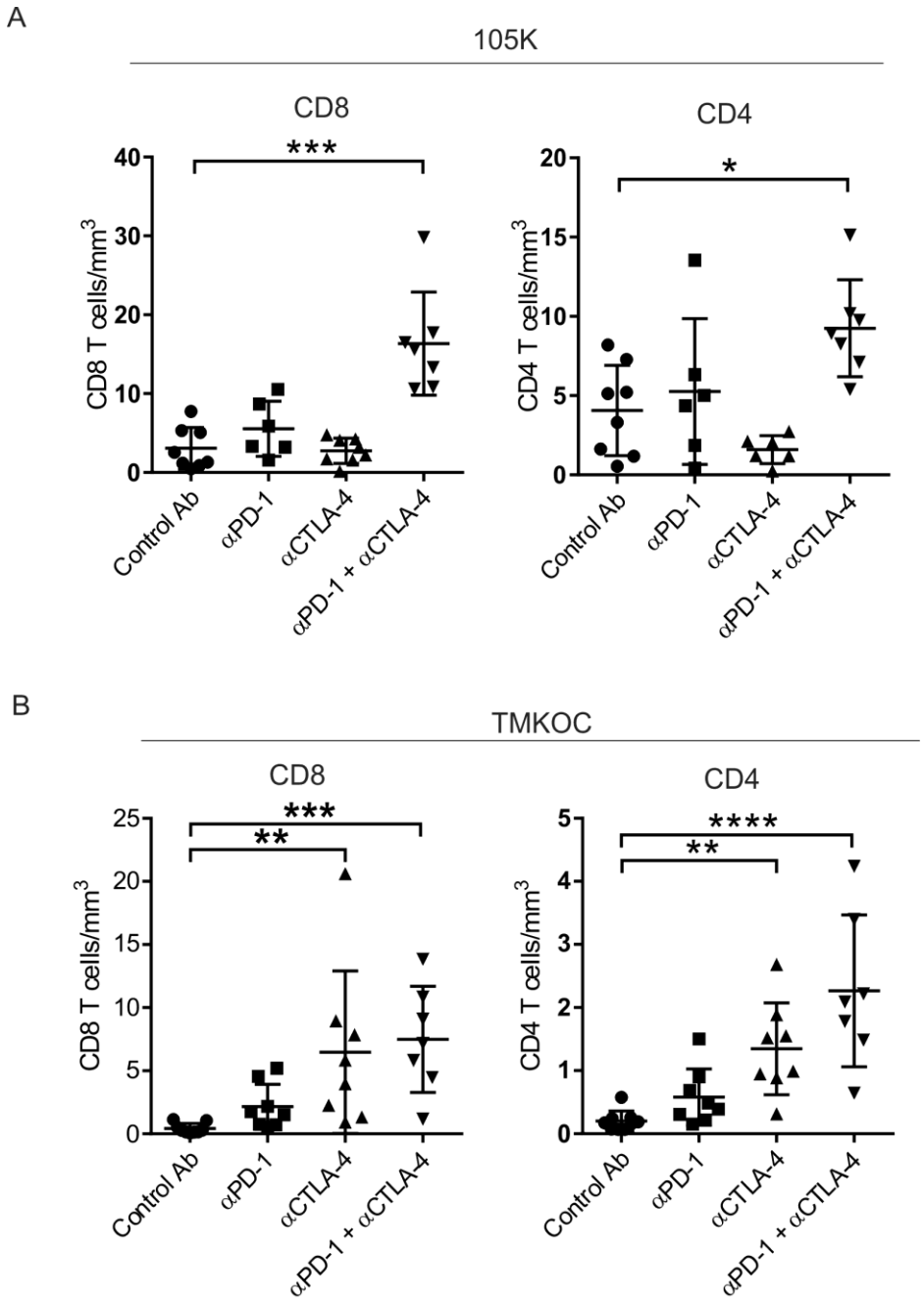

Supplemental Figure 3. PD-1 and CTLA-4 combination blockade increases the number of CD4⁺ and CD8⁺ T cells in TSC2-defcient tumors. Absolute numbers of CD8⁺ or CD4⁺ T cells per cubic millimeter of TSC2-deficient 105K tumors **(A)** and TSC2-deficient TMKOC tumors **(B)** obtained 24 hours following the last treatment as illustrated in Figure 2A (*n* = 6-8 per group). Data are presented as mean ± SD. Statistical significance was determined by non-parametric ANOVA followed by Dunn's multiple comparison test. * $p < 0.05$; ** $p < 0.01$; *** $p < 0.001$; **** $p < 0.0001$.

Figure S4

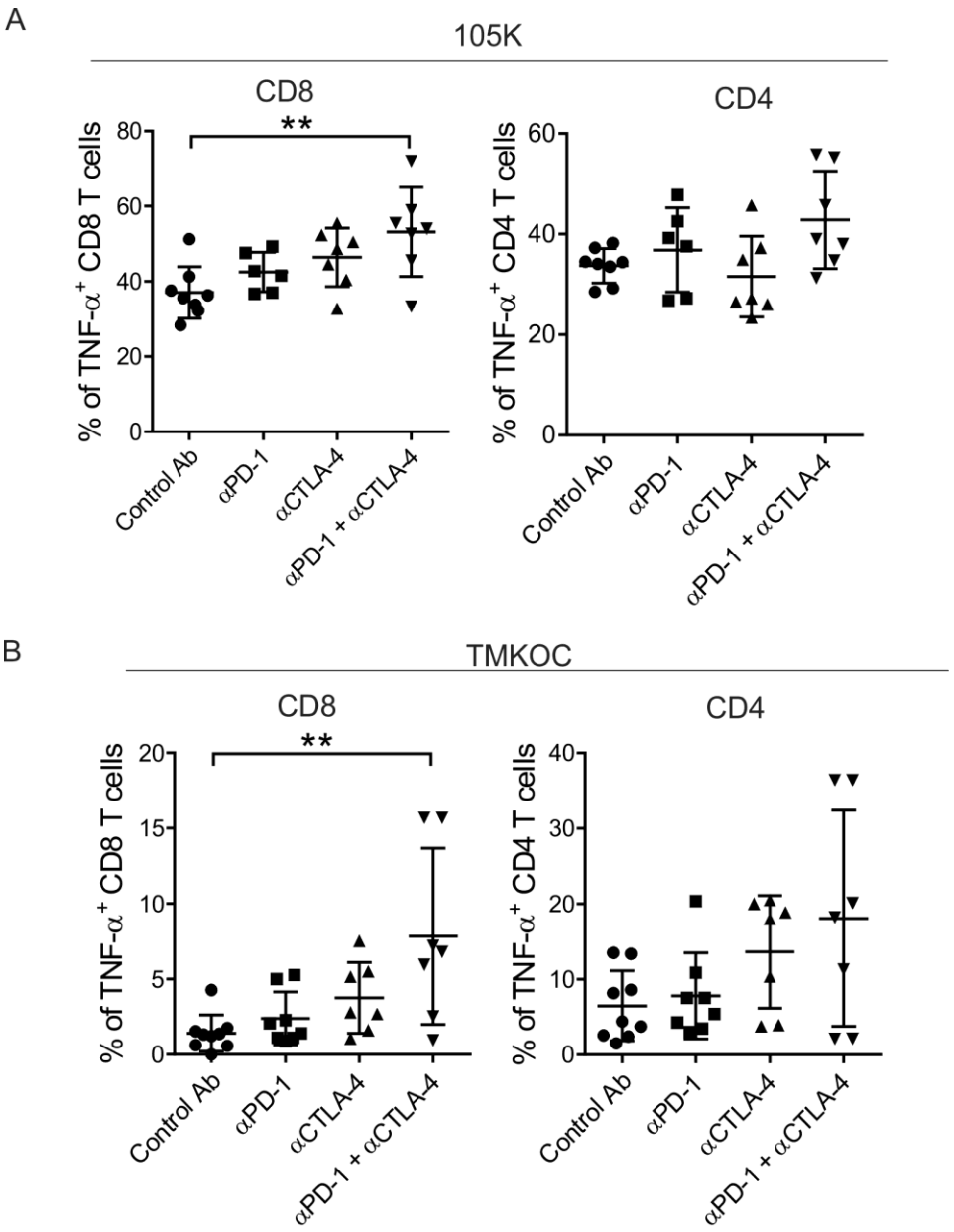

Supplemental Figure 4. PD-1 and CTLA-4 combination blockade increases TNF-α producing CD8⁺ T cells in TSC2-deficient tumors. Tumor-infiltrating lymphocytes (TILs) were purified from subcutaneous 105K **(A)** or TMKOC **(B)** tumors using Ficoll gradient 24 hours following the last treatment as illustrated in Figure 2A. TILs were stimulated with cell stimulation cocktail containing PMA and ionomycin in the presence of GolgiPlug for 4 hours. Cells were fixed using the FoxP3 kit and analyzed by flow cytometry for lymphocyte markers and intracellular TNF-α production for CD8⁺ and CD4⁺ T cells (n = 7-9 per group). Data are presented as mean ± SD. Statistical significance was determined by non-parametric ANOVA followed by Dunn's multiple comparison test. ** $p < 0.01$.

Figure S5

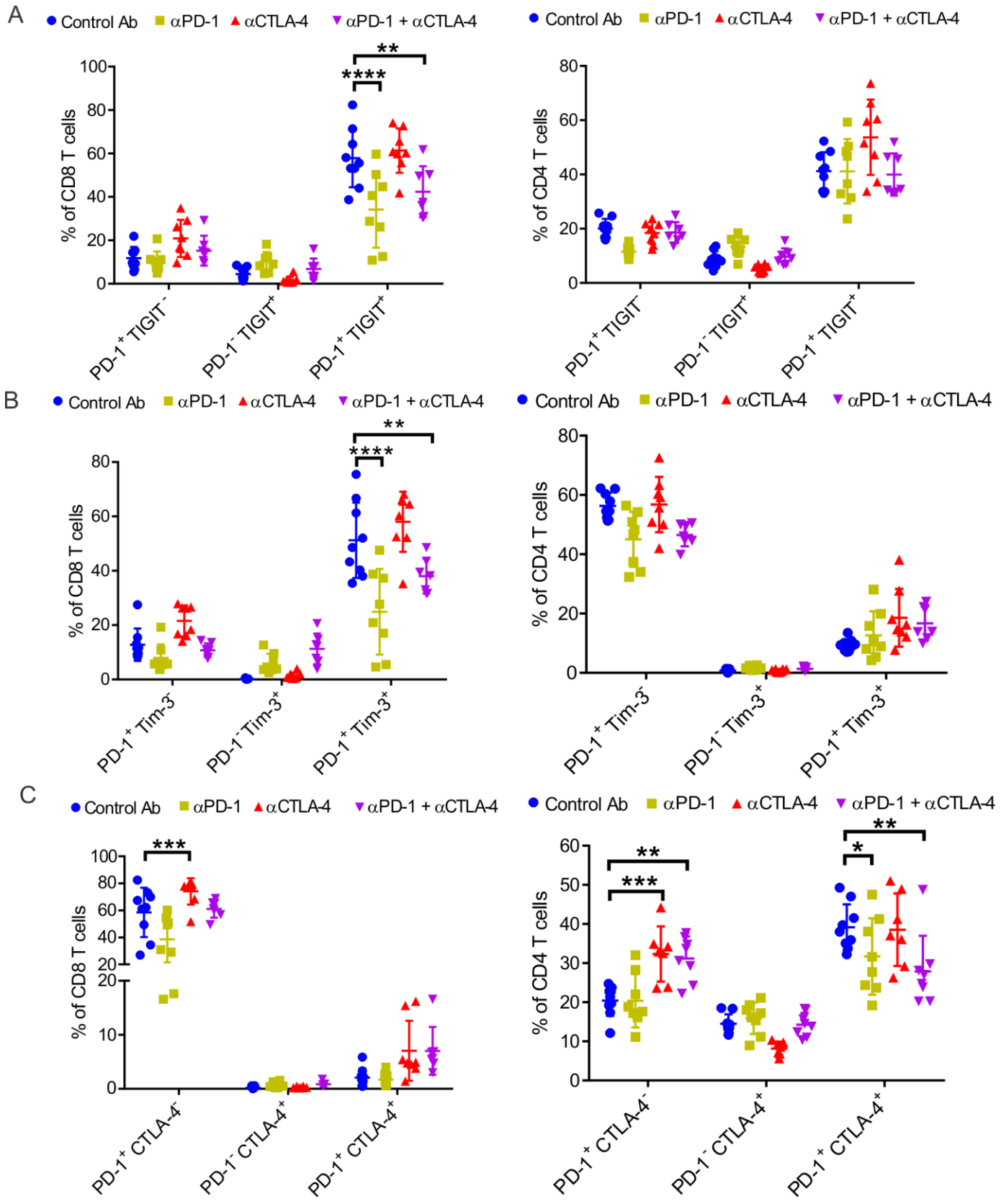

Supplemental Figure 5. PD-1 blockade alone or in combination with CTLA-4 blockade suppress PD-1$^+$TIGIT$^+$ and PD-1$^+$Tim-3$^+$ CD8$^+$ T cells within TSC2-deficient TMKOC tumors. Flow cytometry quantification of the tumor-infiltrating PD-1$^+$ and/or TIGIT$^+$CD8$^+$ or CD4$^+$ T cells **(A)**, PD-1$^+$ and/or Tim-3$^+$CD8$^+$ or CD4$^+$ T cells **(B),** and PD-1$^+$ and/or CTLA-4$^+$CD8$^+$ or CD4$^+$ T cells **(C)** in TSC2-deficient TMKOC tumors 24 hours following the last treatment as illustrated in Figure 2A (n = 7-9 per group). Data are presented as mean ± SD. Statistical significance was determined by two-way ANOVA followed by Holm-Sidak multiple comparison test. * $p < 0.05$; ** $p < 0.01$; *** $p < 0.001$; **** $p < 0.0001$.

Figure S6

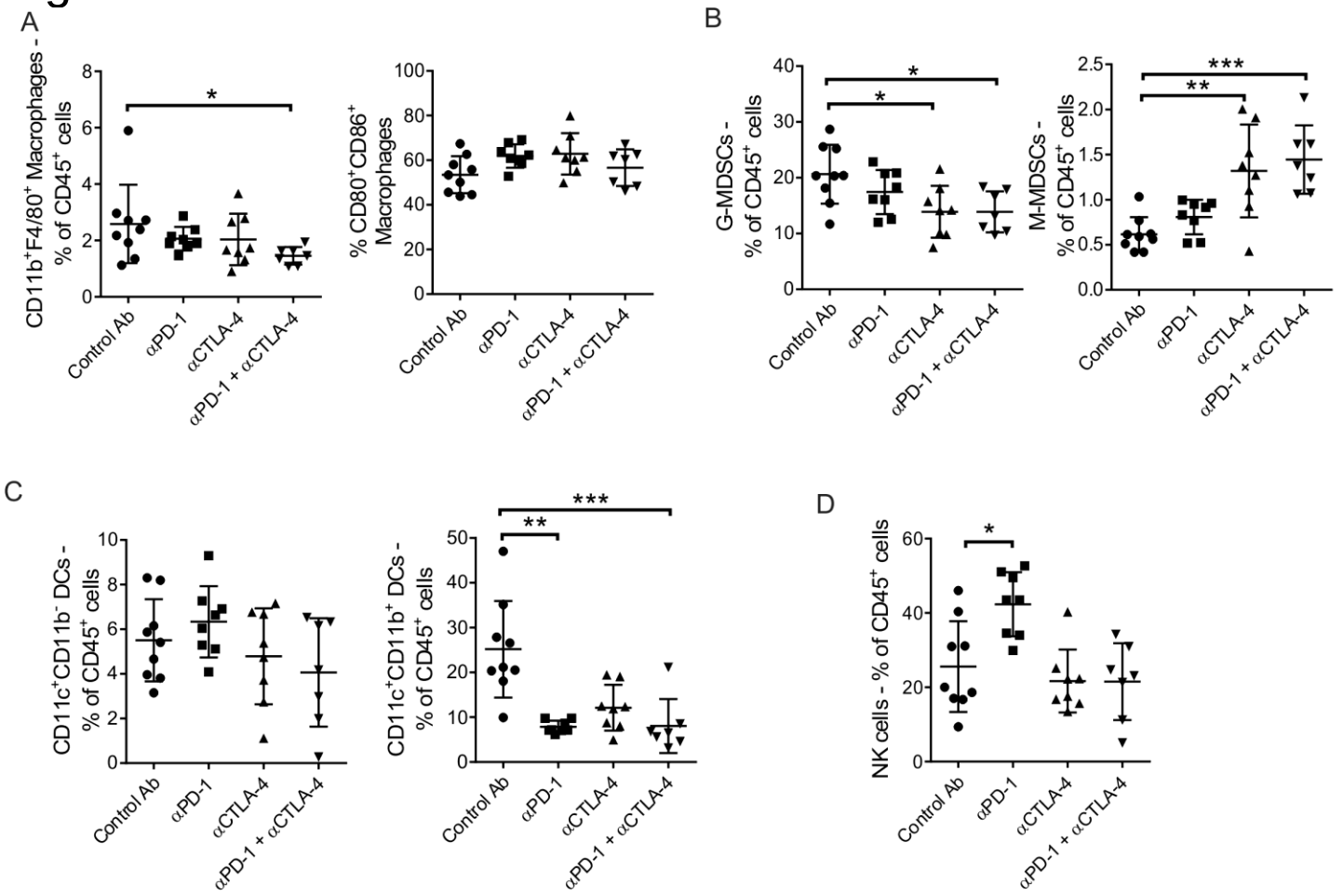

Supplemental Figure 6. PD-1 and CTLA-4 combination blockade decreases CD11b$^+$F4/80$^+$ macrophages, CD11b$^+$Ly6C^{med}Ly6G$^+$ G-MDSCs and regulatory CD11b$^+$ DCs in TSC2-deficient TMKOC tumors. Mice carrying TSC2-deficient TMKOC tumors were treated as illustrated in Figure 2A, Tumor-infiltrating lymphocytes (TILs) were isolated and stained for myeloid lineage and activation markers. Percentage of CD11b$^+$F4/80$^+$ macrophages and CD80$^+$CD86$^+$ macrophages **(A)**, G-MDSCs and M-MDSCs **(B)**, CD11c$^+$CD11b$^-$ DCs and CD11c$^+$CD11b$^+$ DCs **(C)**, NK cells **(D)** within CD45$^+$ cells isolated from TSC2-deficient TMKOC tumors are shown for mice receiving the indicated therapy (n = 7-9 per group). Data are presented as mean ± SD. Statistical significance was determined by non-parametric ANOVA followed by Dunn's multiple comparison test. * $p < 0.05$; ** $p < 0.01$; *** $p < 0.001$

Figure S7

A

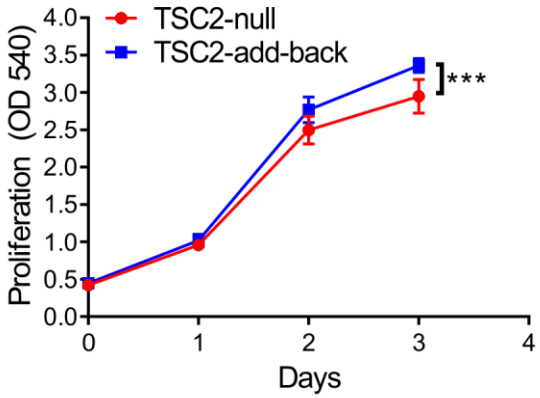

B

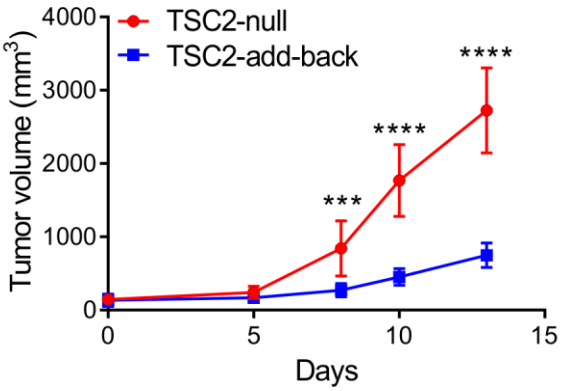

Supplemental Figure 7. TSC2-add-back TMKOC cells grow faster in vitro but slower in *Cd8*$^{-/-}$ mice. (A) Same number of TSC2-null TMKOC or TSC2-add-back TMKOC cells were seeded and cell proliferation was measured by crystal violet staining at 0, 1, 2, 3, days post-seeding. Viable and stained cells were dissolved for OD reading. The results are presented as mean ± SD of three separate experiments. Statistical significance was determined by Student's t-test. **(B)** Growth of TSC2-null or TSC2-add-back TMKOC tumors in *Cd8*$^{-/-}$ mice (n = 10 per group). Data are presented as mean ± SD. Statistical significance was determined by Mann-Whitney U test. *** $p < 0.001$; **** $p < 0.0001$.

Figure 8

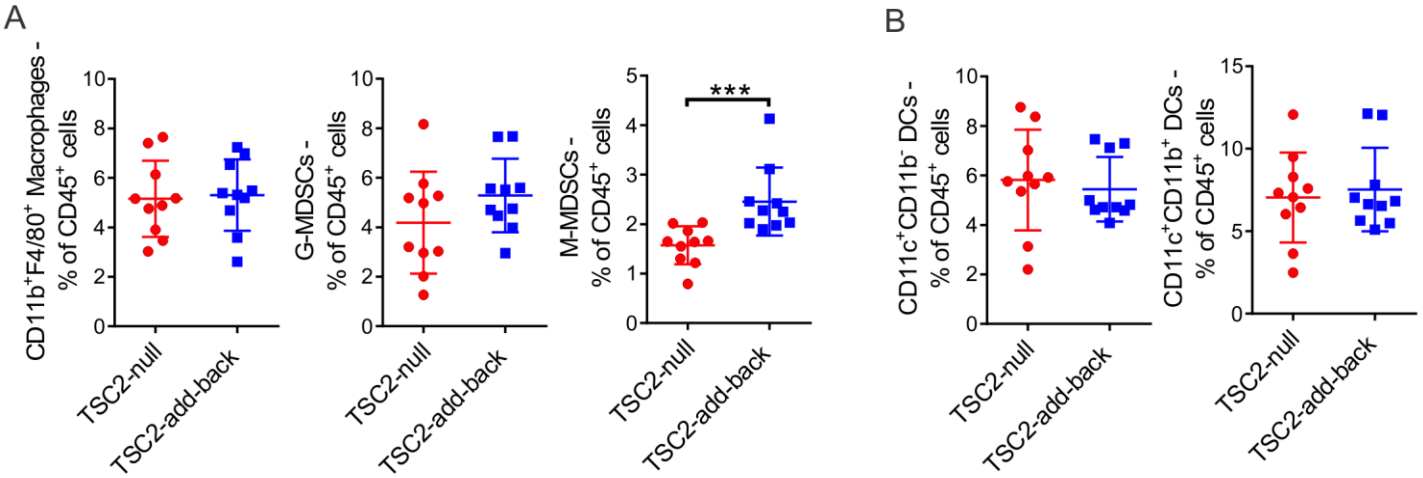

Supplemental Figure 8. TSC2 re-expression increases M-MDSCs but does not change TAMs, G-MDSCs and DCs. Tumor-infiltrating lymphocytes **(**TILs) were isolated and stained for myeloid lineage markers. Percentage of $CD11b^{+}F4/80^{+}$ macrophages, $CD11b^{+}Ly6C^{med}Ly6G^{+}$ G-MDSCs and $CD11b^{+}Ly6C^{+}Ly6G^{-}$ M-MDSCs **(A)** as well as $CD11c^{+}CD11b^{-}$ DCs and $CD11c^{+}CD11b^{+}$ DCs **(B)** within $CD45^{+}$ cells isolated from TSC2-null TMKOC or TSC2-add-back TMKOC tumors are shown (n = 10 per group). Data are presented as mean ± SD. Statistical significance was determined by Mann-Whitney U test. *** $p < 0.001$

Figure S9

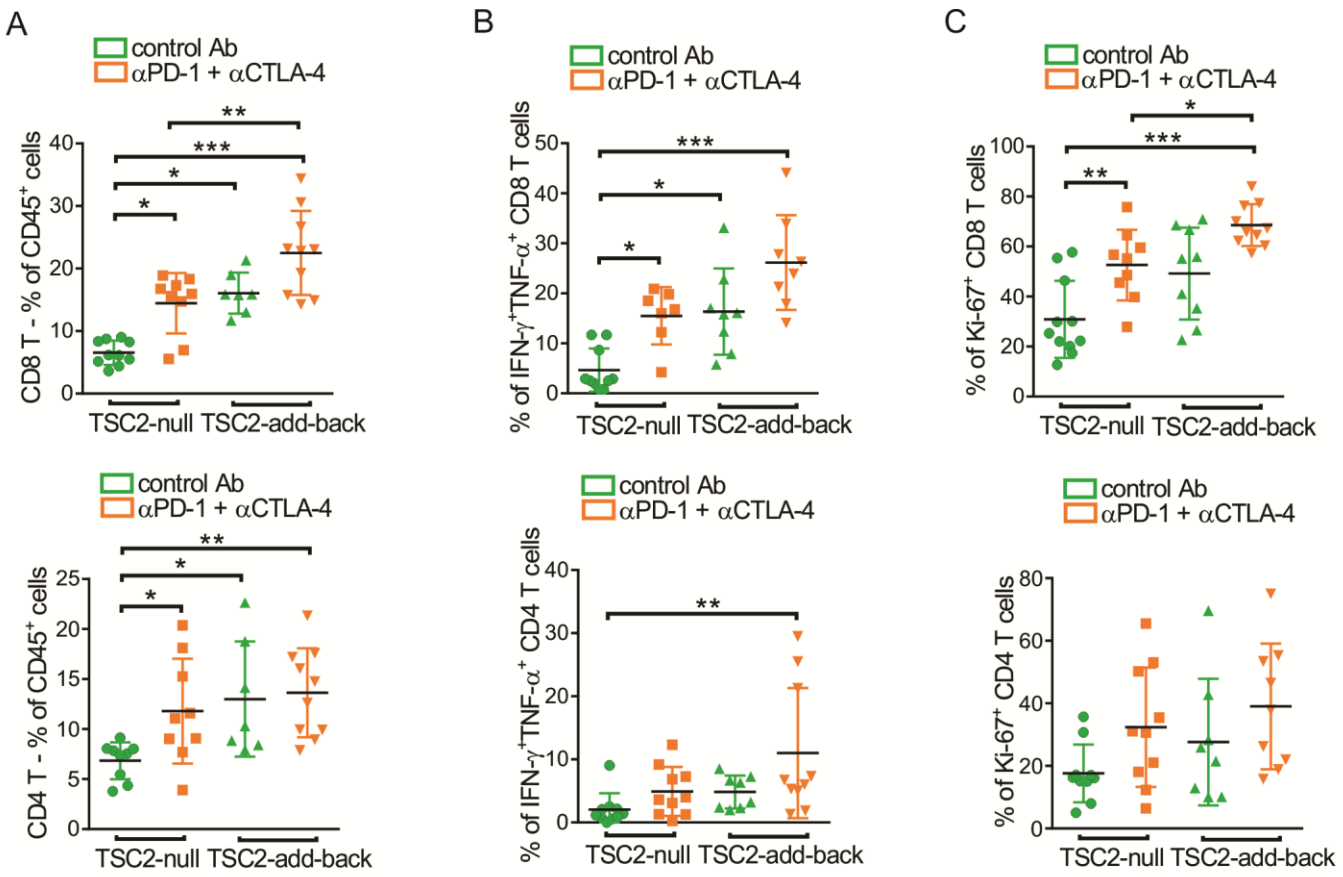

Supplemental Figure 9. TSC2 re-expression promotes infiltration, IFN-γ/TNF-α production and proliferation of T cells following dual PD-1 and CTLA-4 blockade. TILs were purified from subcutaneous TSC2-null and TSC2-add-back TMKOC tumors using Ficoll gradient, 24 hours following the last treatment as illustrated in Figure 9H. Tumor-infiltrating lymphocytes (TILs) were stimulated with cell stimulation cocktail containing PMA and ionomycin in the presence of GolgiPlug for 4 hours. $CD8^+$ and $CD4^+$ T cells were analyzed by flow cytometry for lymphocyte markers **(A)** intracellular IFN-γ and TNF-α production **(B)** and Ki-67 expression **(C)**, (n = 7-10 per group). Data are presented as mean ± SD. Statistical significance was determined by non-parametric ANOVA followed by Dunn's multiple comparison test. * $p < 0.05$; ** $p < 0.01$, *** $p < 0.001$.